

# RADAR MEASUREMENTS OF SMALL DEBRIS FROM HUSIR AND HAX

J. Hamilton<sup>(1)</sup>, C. Blackwell<sup>(2)</sup>, R. McSheehy<sup>(3)</sup>, Q. Juarez<sup>(3)</sup>, P. Anz-Meador<sup>(3)</sup>

<sup>(1)</sup> NASA Johnson Space Center, 2101 NASA Parkway, Houston, TX 77058

<sup>(2)</sup> ERC Inc.-- Jacobs JETS Contract, 2224 Bay Area Blvd, Houston, TX 77058

<sup>(3)</sup> Jacobs, 2224 Bay Area Blvd, Houston, TX 77058

## ABSTRACT

For many years, the NASA Orbital Debris Program Office has been collecting measurements of the orbital debris environment from the Haystack Ultra-wideband Satellite Imaging Radar (HUSIR) and its auxiliary (HAX). These measurements sample the small debris population in low earth orbit (LEO). This paper will provide an overview of recent observations and highlight trends in selected debris populations. Using the NASA size estimation model, objects with a characteristic size of 1 cm and larger observed from HUSIR will be presented. Also, objects with a characteristic size of 2 cm and larger observed from HAX will be presented.

## 1 INTRODUCTION

The NASA Orbital Debris Program Office (ODPO) has been conducting end-to-end orbital debris activities including measurements, modeling, environmental management, and risk assessment since its inception in 1979. The NASA ODPO is the leader in measurements of the orbital debris environment including over 1000 hours annually of radar measurements in addition to optical and in-situ measurements. The radar measurements are designed to sample the debris population in LEO that is too small to maintain in the Space Surveillance Network catalog, but large enough to pose damage risk to operational spacecraft.

The primary source of radar measurements for the office are the Massachusetts Institute of Technology Lincoln Laboratory (MIT/LL) Haystack Ultra-wideband Satellite Imaging Radar (HUSIR) and the Haystack Auxiliary Radar (HAX). The longstanding partnership between MIT/LL and NASA ODPO has existed since the early 1990's. In any given year MIT/LL has sought to provide approximately 1000 hours of radar observations split between HUSIR and HAX per US fiscal year.

An in-depth discussion of the NASA ODPO radar data collection, signal processing, and data analysis on data delivered from MIT/LL is available in "Haystack and HAX Radar Measurements of the Orbital Debris Environment: 2006-2012" [1]

The two radars complement each other. HUSIR, a larger radar with a smaller beam and higher sensitivity, is best suited for measuring smaller debris in the 0.5 to 2.0 cm size range. As the size increases past 3 cm, the sampling geometry favors HAX because it is sensitive enough to detect objects of this size and has a larger detection area which is needed to sample the smaller populations.

## 2 DATA COLLECTION OVERVIEW

The dataset presented in this report was collected from 2006 to 2014 with both radars, HUSIR and HAX. Prior to 2014 HUSIR was known as Haystack or the Long Range Imaging Radar (LRIR), however, the radar underwent significant renovations and upgrades to both hardware and software starting in 2010 and completed in 2014. Both radars are located in Westford, Massachusetts with a Cassegrain focus at the locations found in Table 1 with respect to the 1984 World Geodetic System (WGS 84) Earth model.

Table 1. Radar Coordinates Relative to the WGS 84 Earth Model

Radar	Latitude	Longitude	Altitude
HUSIR	42.623287°	288.511846°	115.69 m
HAX	42.622835°	288.511709°	101.11 m

The sensitivity of each radar is calculated assuming a single pulse on a 1 square meter target at 1000 km. This calculation yields a signal-to-noise ratio (SNR) of 59.2 dB and 40.56 dB for HUSIR and HAX respectively. In terms of characteristic length of debris, this level of sensitivity provides a reliable detection of debris down to below 1 cm for HUSIR and about 3 cm for HAX. Partial failures sometimes reduce the sensitivity which needs to be taken into account when applying the results to update environment models.

All of the orbital debris was collected with the beam parked at 75° elevation and 90° azimuth. The east-staring configuration provides the ability to sample debris in orbits with inclinations between 40 and 140 degrees. The 75° elevation provides the ability to use range-rate to

distinguish between orbit inclinations by measuring the Doppler frequency shift of the returned radar signal. In this report, a circular orbit assumption is used to calculate an approximate value for inclination. In reality, a group of objects with the same inclination but various eccentricities will appear to spread across a range of inclinations in the plots. Due to low SNR on most detections Doppler range rates provide a better estimate for inclination than a monopulse derived estimate.

Signal processing was accomplished using the Orbital Debris Analysis System with 16-pulse non-coherent integration. To declare a valid detection the SNR must be greater than 5.45 dB and within the 3-dB beamwidth.

A summary of the hours of observation and the number of detections for Haystack/HUSIR is presented in Tab. 2 and for HAX in Tab. 3. Additional data from these radars were collected at other orientations for specific campaigns, including low elevation staring south to observe lower inclination orbits, but results from those campaigns are not included in this paper.

Table 2. Summary of HUSIR Detections by Year

Year	# of Hours Observed	# of Detections
2006	104.89	90
2007	198.87	184
2008	332.24	352
2009	375.9	347
2010	670.91	628
2014	263.01	332

Table 3. Summary of HAX Detections by Year

Year	# of Hours Observed	# of Detections
2006	0	0
2007	431.18	345
2008	463.57	490
2009	467.68	484
2010	85.45	88
2011	877.52	904
2012	1167.59	1279

2013	985.11	1074
2014	696.77	672

## 2.1 The NASA Size Estimation Model (SEM)

The NASA SEM was developed to relate RCS to the physical size of a debris fragment on orbit. Size refers to the characteristic length of an object, which is defined as the average of the largest dimensions for an object measured along three orthogonal axes. It is a simple model for one-to-one RCS-to-size mapping and does not provide an uncertainty estimate for the derived size distribution, nor does it take into account the specific distribution of RCS values for a given size or specific materials.

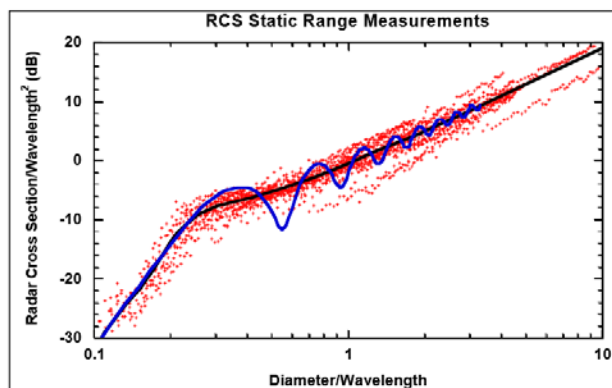


Figure 1. The NASA Size Estimation Model

In Fig. 1 the NASA SEM model polynomial fit (smooth curve) is plotted as a function of scaling parameters, while the oscillating line is the RCS for a spherical conductor. Results of RCS measurements on 39 representative debris objects over the frequency range 2.0–18 GHz (15–1.67-cm wavelength) are shown by points, where each point represents an average RCS over many orientations for a single object measured at a single frequency.

This paper uses the NASA SEM to estimate sizes. A current NASA ODPO project, DebrisSat, is working to eventually replace the SEM with results from controlled hypervelocity testing on modern spacecraft hardware.

## 3 ENVIRONMENT EVOLUTION

### 3.1 Significant Debris Events in Space

Between the beginning of the US Fiscal Year (FY)06 and the end of FY14 39 breakup events and 13 anomalous events were observed. Breakup events are usually characterized by the energetic separation of fragments

from the parent body and, often, a large ensemble of pieces. Anomalous events are usually characterized by low energy fragment separation, in some cases likely the shedding of single objects and multi-layer insulation (MLI) blankets; this category may include events whose fragments are identifiable but with no obvious production mechanism, *e.g.* the apparent production of coolant droplets by the Cosmos 1818 and 1867 *Plazma-A* reactor test spacecraft. Whereas breakup events are indicative of the resident space object (RSO) population's effect on the environment, it has been suggested that anomalous events may be indicative of the environment's effect on the RSO population. Both categories may experience multiple events for the same RSO, though this is much more common in anomalous event parents. Some RSOs have experienced both anomalous and breakup events. With the exception of the *Plazma-A* spacecraft, anomalous events may not necessarily produce significant numbers of small debris and these are not considered further in this work.

Of the 39 breakup events, one was in Geosynchronous orbit (GEO) and is not relevant to this work; seven events were in GEO transfer orbits and 11 were in Medium transfer orbits; and 20 were in low Earth orbit (LEO), these latter offering the highest probability of observation. Four events account for over 83% of the total ensemble of cataloged debris associated with these breakup events. However, one large event (Cosmos 2421) had no long term effect on the environment due to the source, the area-to-mass distribution of the fragments, and the relatively low altitude of the event. Three events, therefore, account for almost 77% of all debris generated in this time span: the People's Republic of China (PRC) Anti-Satellite (ASAT) vehicle test against the PRC Fengyun-1C LEO weather spacecraft and the inadvertent collision of the derelict Russian Cosmos 2251 and active US commercial Iridium 33 communication spacecraft. FY-1C was in a heavily populated polar orbit at 865 km altitude and an inclination of 98.8°. The second event occurred on 10 February 2009 at an altitude of 789 km. Iridium 33 and Cosmos 2251 were in orbital inclinations of 86.4° and 74° respectively. The immediate effect on the large (> approximately 10 cm characteristic size) object environment is shown in Fig. 2.

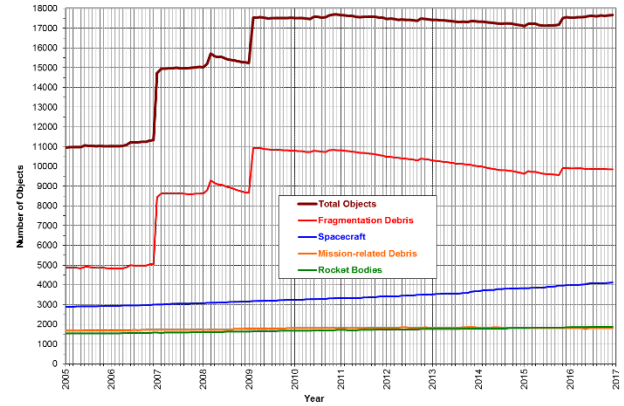


Fig. 2. The monthly number of objects by type, derived from the US Satellite Catalog. Note that cataloged objects associated with an earlier breakup are deposited at breakup time in this figure, not at the time they entered the catalog. Graphic courtesy Mr. J. Opiela, Jacobs.

Immediately after these events, the ODPO simulated the fragment clouds using the NASA Standard Satellite Breakup Model (Ref. 2) and custom radar campaign planning software and conducted special measurements of the small object (< approximately 10 cm) component using those predictions. These are summarized in Ref. 1, Section 8.1.

Now, over a decade after the PRC ASAT test, these three major debris clouds continue to influence the LEO environment. The spatial density distribution of the US Satellite Catalog (epoch 20 March 2017), with these debris clouds displayed individually, is shown in Fig. 3.

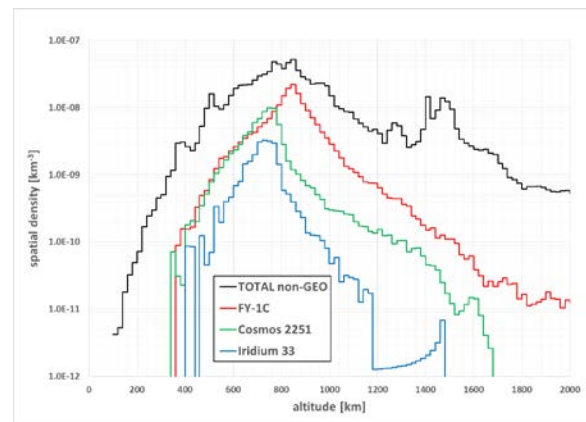


Fig. 3. The spatial density of objects passing through altitudes below 2000 km, with three major debris clouds highlighted. Note that in some 20 km altitude bins, such as 860-880 km, the FY-1C cloud alone accounts for 43% of the effective (time-weighted) density resident in that bin.

The corresponding distribution in inclination is shown in Fig. 4 for the FY1C breakup. In this figure, the change in inclination with respect to the parent body is shown.

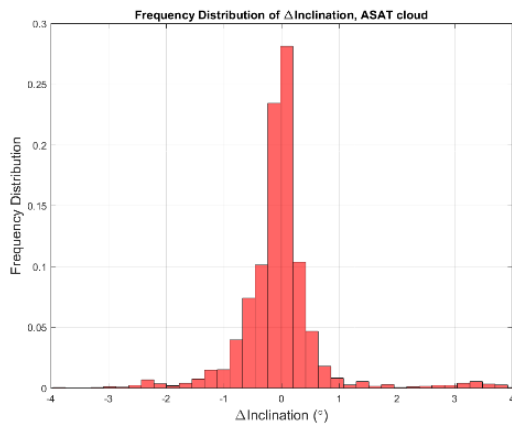


Fig. 4. FY1C cloud inclination distribution for US Satellite Catalog data. Courtesy Mr. D. Vavrin, GEO Controls--Jacobs JETS Contract.

Unfortunately, due to the nature of the radar's statistical sampling of the debris cloud's small size component, figures 3 and 4 do not readily lend themselves to a bias-free, deterministic filter by which the cloud debris may be unequivocally identified in the general debris population. Rather, statistical methods must be employed to extract the cloud's small particle component. Ideally, this methodology minimizes or reduces the potential filter biases by using directly-observed variables, *e.g.* range, range rate, noise floor, and signal-to-noise ratio. Templates may be used to model the evolution of the debris cloud to any epoch for comparison against measurements taken at that epoch. The cloud component is then extracted in a statistical manner using Maximum Likelihood Estimation in a Bayesian framework (Ref. 3). This work is being currently conducted in the development of the data-driven ODPO Orbital Debris Engineering Model (ORDEM) version 3.1, and will be reported upon in a future paper. An exemplar template for the PRC ASAT cloud, as predicted to be viewable by the HUSIR radar in 2014, is shown in Fig. 5.

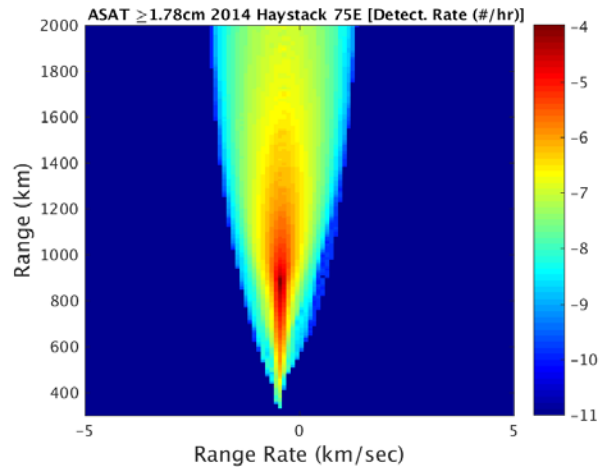


Fig. 5. The range-range rate density distribution of the modeled PRC ASAT debris cloud, predicted for the HUSIR radar in 2014. Density scaling is  $\log_{10}(\text{detection rate } [\text{hr}^{-1}])$ . Graphic courtesy of Dr. Y.-L. Xu, University of Texas at El Paso--Jacobs JETS Contract.

### 3.2 Regions of Interest

The majority of NASA operational spacecraft operate in the LEO altitude region observable by HUSIR and HAX. The ODPO provides general mission support by providing mission risk assessments, environmental management, and coordination with the US Government and international bodies to the level of the United Nations. Radar measurements are fundamental to understanding and modeling the LEO environment, and models enable many aspects of general mission support. In particular, the HUSIR/HAX data set provide key spatial and temporal measurements of the dynamic LEO environment for national and international mission support, including the International Space Station, the Hubble Space Telescope, and the Earth Observing System spacecraft.

We highlight the temporal effects of these events by dividing our analysis into four distinct eras:

- Pre-events Environment consists of data taken before the Chinese ASAT test on 11 January 2007
- Post-ASAT, Pre-Collision consists of data taken between 12 January 2007 and 10 February 2009
- Post-ASAT Test, Post-Collision consists of data taken between 11 February 2009 and 30 September 2009
- Modern Environment consists of data taken between 1 October 2013 and 30 September 2014 (US FY 2014).

The gap between the third and fourth eras is a result of the Haystack/HUSIR upgrade. Data exists for this time period taken by the HAX radar but it is not presented in this analysis.

## 4 RADAR RESULTS

The results are presented as comparisons of the four eras for each radar. The parameters presented include flux, altitude, inclination, and size distribution. Flux is represented in units of the number of detections over a year for each square meter of detection area. With each data bin there is an uncertainty due to the sample size relative to the total population. Plots presented here include only the measurement results. Overlaying the uncertainty in the plots can be useful to help in drawing conclusions from the data, but it also clutters up the plots, particularly when comparing multiple sets of data. The uncertainties will be considered as the data is applied to environment models.

### 4.1 HUSIR Measurements

The cumulative size distribution for HUSIR data is shown in Fig. 6. It shows a clear progression of increasing debris population from one era to the next.

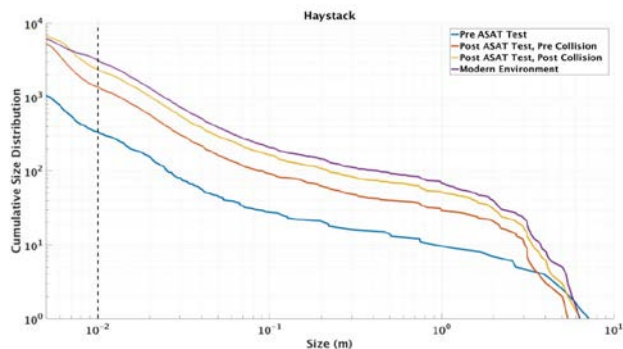


Figure 6. HUSIR cumulative size distribution

In subsequent plots for HUSIR, all data with an SEM estimate of 1 cm or greater are included. Although there is data below 1 cm, indicated by the vertical dotted line, the detections start to fall off as a function of altitude as the size decreases.

Fig. 7 shows the flux from HUSIR distributed in 50 km altitude bins.

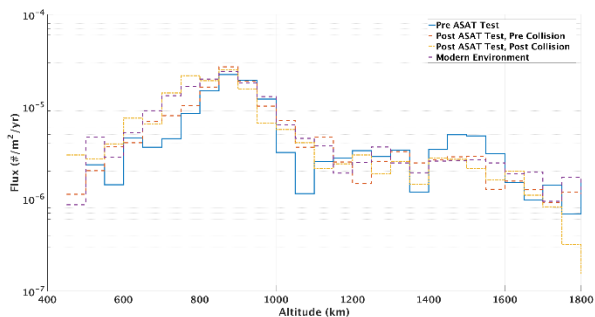


Figure 7. HUSIR 1cm Flux vs. Altitude

The solid blue line represents the first era. Increases in the population are evident below 900 km and from 1000 to 1150 km. The apparent decrease in population near 1500 km after the first era may be due to variations from smaller sample sizes at those altitudes.

When the flux is plotted as a function of inclination in Fig. 8, there is a general increasing trend but this varies by inclination.

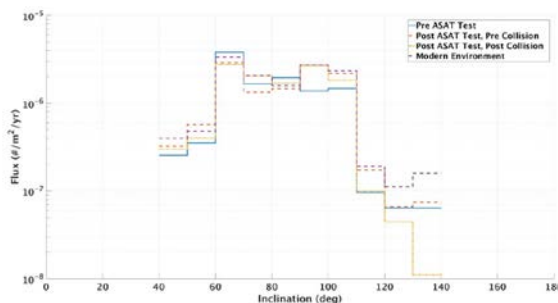


Figure 8. HUSIR 1cm Flux vs. Inclination

The effect of the ASAT test is clearly evident in the 90-100 degree and 100-110 degree bins. There also appears to be an increase in the 120-130 degree bin which would naively imply that some objects generated from the test were given a significant eccentricity from the event. In reality, the assumption of circular orbits imposed by the analysis software tends to re-map eccentric orbits into inclinations (and, potentially, other orbit shape and orientation variables). However, the low sample populations in this bin make it harder to draw conclusions.

Fig. 9 shows the distribution of HUSIR detections with a characteristic size equal to or greater than 1 cm as a scatter plot of altitude versus inclination.

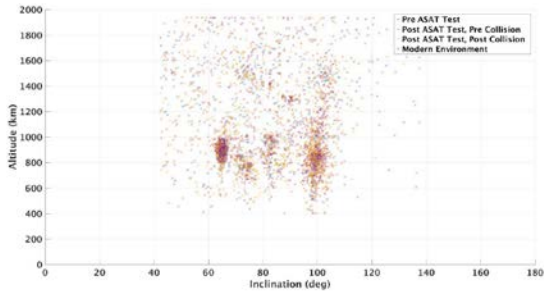


Figure 9. HUSIR 1cm Altitude vs. Inclination

Several clumps indicate which orbits are more cluttered than others. For example, the large clump from 62° to 68° inclination is largely due to a population of sodium-potassium (NaK) droplets that has been mostly stable for years prior to the beginning of this data set. As new events add debris to various orbits, it becomes increasingly difficult to attribute specific objects to individual events. The ASAT test was the largest of multiple sources that have contributed debris in the slightly retrograde sun-synchronous orbits.

#### 4.2 HAX Measurements

The results for HAX are presented in a similar manner as the results from HUSIR. HAX sensitivity is significantly less than HUSIR. The HAX cumulative size distribution plot in Fig. 10 shows a similar increase in the debris population over time that was seen in the HUSIR data.

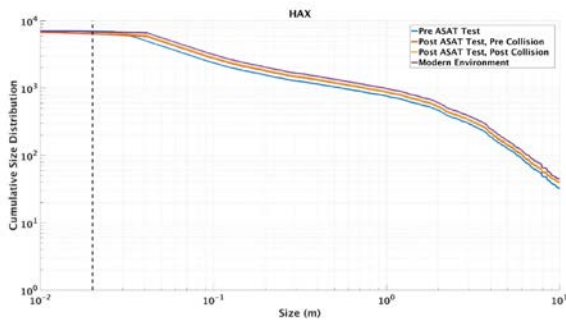


Figure 10. HAX cumulative size distribution

The vertical dotted line at 2 cm marks the characteristic size cut-off that is used for the remainder of the HAX

plots. Even with the cutoff, there is a falloff in sensitivity with altitude which has to be considered. Also, a degradation in the performance of the HAX radar starting in 2012 further complicates the analysis.

Fig. 11 displays the HAX radar flux in 50 km altitude bins. The solid blue line shows the first era. Detections increase relative to the first era in similar altitude bins to the HUSIR although there are some differences.

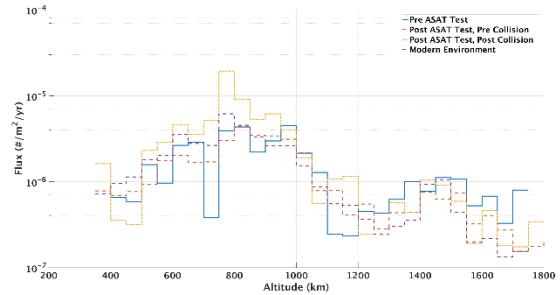


Figure 11. HAX 2cm Flux vs. Altitude

The differences may be a reflection of a difference in the environment population since HAX is not detecting the 1 cm objects in the HUSIR data, or it may be a result of variation due to small sample sizes. Further analysis will put a bound on the sampling challenge.

In Fig. 12, the flux is divided into 10° inclination bins. The results show a complex mixture of increases and decreases.

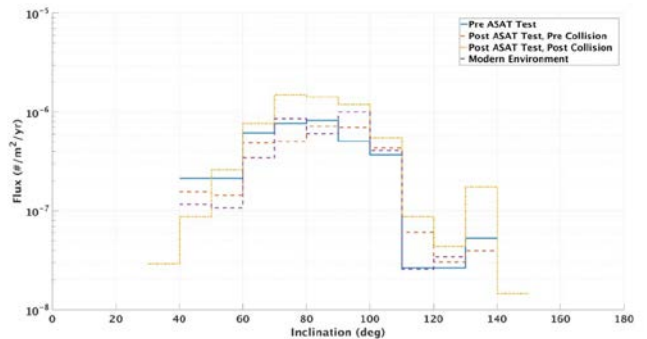


Figure 12. HAX 2 cm Flux vs. Inclination

The scatter plot of HAX detections in altitude versus inclination, Fig. 13, shows many of the same groups that were seen in the HUSIR data. Most of the NaK population is too small to be detected by HAX.

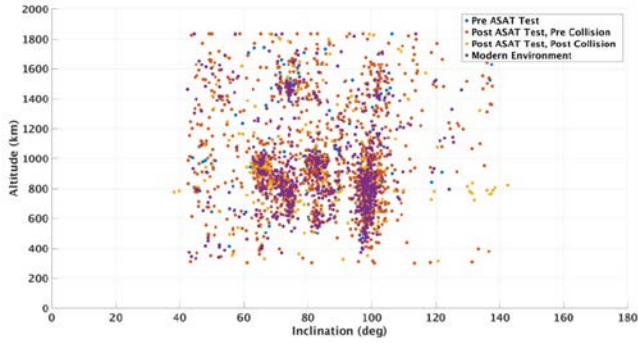


Figure 13. HAX 2 cm Altitude vs. Inclination

Detections from the Iridium 33 and Cosmos-2251 clouds appear more pronounced in this data. The cloud at 1500 km and 74° inclination is also prominent.

## 5 DISCUSSION

Radar measurements that count objects passing through a small beam have limited information about each object. The primary parameters available to measure are range, range-rate, and RCS. There is not enough information to accurately determine the state vector of each object. Altitude can be directly calculated from range and angle information, but indirect parameters, such as characteristic size and orbit inclination, must be estimated using some assumptions.

Real measurements have error sources that may cause results to differ from a model that assumes an ideal sensor. The radar mode of ORDEM 3.0 is an example of a model that predicts what an ideal radar would detect for a given year. The model outputs predicted flux in 50 km altitude bins at specific debris sizes. Fig. 14 shows a comparison of the 2014 HUSIR 1 cm characteristic size results to ORDEM 3.0 predictions for 1 mm, 1 cm, and 10 cm sizes for the same year.

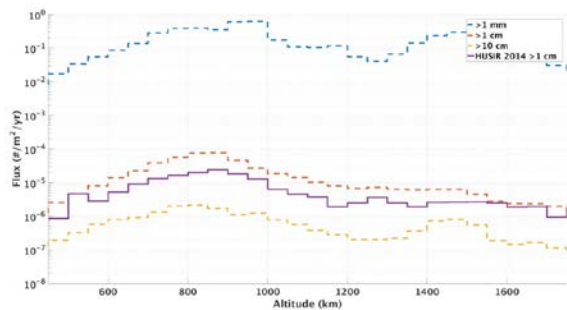


Figure 14. Comparing HUSIR and ORDEM 3.0

The radar measurements show a mostly consistent pattern of detecting fewer objects at each altitude than predicted

by the model. The model is a forecast of the environment from a previous era based upon available measurements and assumptions of how events would change the environment over time. One of those assumptions includes a projection of occasional major events such as the ones mentioned in this paper. These events cause a sudden spike in the debris population in the year of the event. Since the model cannot accurately predict when a major event will occur, it has to average the effects of such events over time. This may cause a given year to predict high or low, depending upon when the last major event occurred. These radar measurements will be used as one of the sources of information to update ORDEM 3.0.

Fig. 15 shows the same ORDEM 3.0 predictions compared to the 2014 HAX measurements.

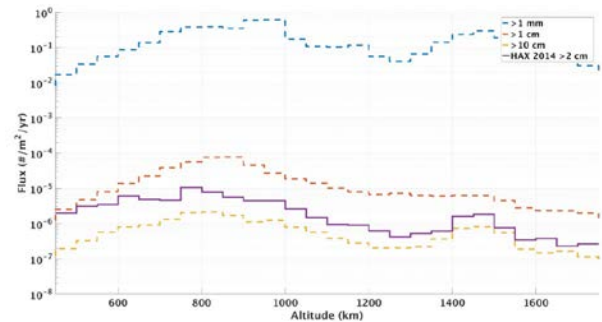


Figure 15. Comparing HAX and ORDEM 3.0

At lower altitudes, the HAX results are closer to the 1 cm predictions but fall towards the 10 cm prediction as altitude increases. This is not surprising because the radar sensitivity is dropping with altitude. By 1800 km, the detection capability is down to about 7 or 8 cm.

## 6 CONCLUSIONS

Measurements from HUSIR and HAX indicate a strong trend towards increasing debris populations in LEO over the observation time period from 2006 to 2014. Many events, large and small, contributed to this trend. This paper presented a summary of the direct radar measurements that represent samples of the total debris population. The results presented here are a major source of information for updating LEO space debris environment models and predictions. To correctly apply these results, the NASA ODPO will carefully examine the capabilities and limitations of each radar, and the sample populations observed.

## 7 REFERENCES

1. Haystack and HAX Radar Measurements of the Orbital Debris Environment: 2006-2012, <https://ston.jsc.nasa.gov/collections/trs/techrep/TP-2014-217391.pdf>
2. Johnson, N.L., P.H. Krisko, J.-C. Liou, *et al.* "NASA's New Breakup Model of EVOLVE 4.0". Adv. Space Res. **28**, No. 9 (2001): 1377-84.
3. Xu, Y.-L., M. Horstman, P.H. Krisko, *et al.* "Modeling LEO orbital debris populations for ORDEM2008". Adv. Space Res. **43** (2009): 769-82.